







10.24425/acs.2025.156310

Archives of Control Sciences
Volume 35(LXXI), 2025
No. 3, pages 561–585

A new 5-D highly hyperchaotic system with a line equilibrium, its bifurcation analysis, multistability and electronic circuit simulation

Sundarapandian VAIDYANATHAN , Fareh HANNACHI , Irene M. MOROZ ,
Mohamad Afendee MOHAMED , Aceng SAMBAS ,
Chittineni ARUNA  and A. Raghava RAJU

In this research work, we propose a new 5-D highly hyperchaotic system with three quadratic nonlinear terms. A novel feature of the new hyperchaotic system is that it has the maximal Lyapunov exponent (MLE) given by $L_1 = 10.5374$ which implies that the proposed hyperchaotic system has high complexity. Another novel feature of the new hyperchaotic system is that the system exhibits a line of equilibrium points, which shows that the new hyperchaotic system has hidden attractors. We carry out a detailed bifurcation analysis of the new hyperchaotic system with a line equilibrium. Using Multisim, we build an electronic circuit of the new 5-D hyperchaotic system with a line equilibrium. As a control application, we use integral

Copyright © 2025. The Author(s). This is an open-access article distributed under the terms of the Creative Commons Attribution-NonCommercial-NoDerivatives License (CC BY-NC-ND 4.0 <https://creativecommons.org/licenses/by-nc-nd/4.0/>), which permits use, distribution, and reproduction in any medium, provided that the article is properly cited, the use is non-commercial, and no modifications or adaptations are made

S. Vaidyanathan (corresponding author, e-mail: sundar@veltech.edu.in) is with Centre for Control Systems, Vel Tech University, 400 Feet Outer Ring Road, Avadi, Chennai-600062 Tamil Nadu, India and Faculty of Information and Computing, Universiti Sultan Zainal Abidin Terengganu, Malaysia.

F. Hannachi (e-mail: fareh.hannachi@univ-tebessa.dz) is with Department of Management Sciences, Echahid Cheikh Larbi Tebessi University, Route de Constantine, 12022, Tebessa, Algeria.

I.M. Moroz (e-mail: Irene.Moroz@maths.ox.ac.uk) is with Mathematical Institute, University of Oxford, Andrew Wiles Building, ROQ, Oxford OX2 6GG, UK.

M.A. Mohamed (e-mail: mafendee@unisza.edu.my) is with Faculty of Information and Computing, Universiti Sultan Zainal Abidin, Terengganu, Malaysia.

A. Sambas (e-mails: acengsambas@unisza.edu.my, acengs@umtas.ac.id) is with Faculty of Informatics and Computing, Universiti Sultan Zainal Abidin, Gong Badak, 21300, Terengganu, Malaysia and Department of Mechanical Engineering, Universitas Muhammadiyah Tasikmalaya, Jawa Barat 46196, Indonesia.

C. Aruna (e-mail: aruna.cse@kitsguntur.ac.in) is with Department of Computer Science and Engineering, KKR & KSR Institute of Technology and Sciences, Vinjanampadu, Vatticherukuru Mandal, Guntur-522017, Andhra Pradesh, India.

A.R. Raju (e-mail: raghavaraju@kitsguntur.ac.in) is with Department of Electronics and Communication and Engineering, KITS Akshar Institute of Technology, NH-16, Yanamadala, Guntur-522019, A.P., India.

Received 14.01.2025.

sliding mode control (ISM) to achieve global asymptotic stabilization of the new 5-D highly hyperchaotic system with a line equilibrium. Lyapunov control theory has been used to establish the stabilization results for the new 5-D hyperchaotic system. MATLAB simulation results are shown to illustrate the main results of this research work.

Key words: hyperchaos, hyperchaotic systems, line equilibrium, bifurcation, circuit design, stabilization, sliding mode control

1. Introduction

Hyperchaotic systems are defined as nonlinear dynamical systems with two or more positive Lyapunov exponents [1]. Hyperchaotic systems have many engineering applications such as cryptography [2, 3], memristive systems [4–6], robotics [7], FPGA design [8, 9], etc.

Chaotic or hyperchaotic systems with an unstable equilibrium are said to possess self-excited attractors [10]. Chaotic or hyperchaotic systems with no equilibrium point or a stable equilibrium point or with infinitely many equilibrium points are said to possess hidden attractors [10].

In this research work, we propose a new 5-D highly hyperchaotic system with three quadratic nonlinear terms. A novel feature of the new hyperchaotic system is that it has the maximal Lyapunov exponent (MLE) given by $L_1 = 10.5374$ which implies that the proposed hyperchaotic system has high complexity. Another novel feature of the new hyperchaotic system is that the system exhibits a line of equilibrium points, which shows that the new hyperchaotic system has hidden attractors.

Bifurcation analysis helps to understand the various qualitative features of chaotic or hyperchaotic systems [11, 12]. We carry out a detailed bifurcation analysis of the new hyperchaotic system with a line equilibrium.

Using Multisim, we build an electronic circuit of the new 5-D hyperchaotic system with a line equilibrium. Electronic circuit design of chaotic or hyperchaotic systems is very useful for the practical, real-world applications of the systems [13–15].

As a control application, we use integral sliding mode control to achieve global asymptotic stabilization of the new 5-D hyperchaotic system with a line equilibrium. Integral sliding mode control (ISM) is an improved form of the sliding mode control (SMC). ISM is a robust and powerful control technique and the system motion under integral sliding mode has a dimension equal to that of the state space [16]. Lyapunov control theory [17] has been used to establish the synchronization results for the new 5-D hyperchaotic system. MATLAB simulation results are shown to illustrate the main results of this research work.

2. A new 5-D hyperchaotic system with a line equilibrium

In this research paper, we propose a new 5-D system with the dynamics:

$$\begin{cases} \dot{x}_1 = a(x_2 - x_1) + x_2x_3 + x_3 + x_4 + x_5, \\ \dot{x}_2 = cx_2 - x_1x_3 + x_4 + x_5, \\ \dot{x}_3 = x_1x_2 - bx_3, \\ \dot{x}_4 = -p(x_1 + x_2), \\ \dot{x}_5 = -x_1. \end{cases} \quad (1)$$

Here, $X = (x_1, x_2, x_3, x_4, x_5)$ is the state vector and a, b, c, p are bifurcation parameters. In this paper, we establish that the new 5-D system (1) has a 5-D hyperchaotic attractor with a line equilibrium for the values of system parameters taken as follows:

$$a = 49, \quad b = 8, \quad c = 180, \quad p = 6. \quad (2)$$

For numerical simulations, we take the initial state as $x_1(0) = 0.2, x_2(0) = 0.1, x_3(0) = 0.2, x_4(0) = 0.1$ and $x_5(0) = 0.2$. We take the bifurcation constants as given in Eq. (2). Then the Lyapunov exponents (LE) of the 5-D system (1) were evaluated for $T = 1E4$ seconds as

$$L_1 = 10.5374, \quad L_2 = 0.0729, \quad L_3 = 0.0131, \quad L_4 = 0, \quad L_5 = -67.6213. \quad (3)$$

The 5-D system (1) is hyperchaotic since it exhibits 3 positive LE values and it is also highly hyperchaotic since its maximal Lyapunov exponent (MLE) is a high value given by $L_{\max} = L_1 = 10.5374$.

Moreover, the Lyapunov dimension of the hyperchaotic system (1) is determined as follows:

$$D_L = 4 + \frac{L_1 + L_2 + L_3 + L_4}{|L_5|} = 4.1571 \quad (4)$$

which is a high value. This shows that the highly hyperchaotic system (1) possesses high complexity.

The balance points of the 5-D system (1) are got by solving the following system of equations:

$$a(x_2 - x_1) + x_2x_3 + x_3 + x_4 + x_5 = 0, \quad (5a)$$

$$cx_2 - x_1x_3 + x_4 + x_5 = 0, \quad (5b)$$

$$x_1x_2 - bx_3 = 0, \quad (5c)$$

$$-p(x_1 + x_2) = 0, \quad (5d)$$

$$-x_1 = 0. \quad (5e)$$

From (5e), $x_1 = 0$. Substituting $x_1 = 0$ in (5d), we get $x_2 = 0$.

Substituting $x_1 = x_2 = 0$ in (5c), we get $x_3 = 0$.

Finally, substituting $x_1 = x_2 = x_3 = 0$ into (5a) and (5b), we get $x_4 + x_5 = 0$.

Thus, the new 5-D hyperchaotic system (1) has a line of equilibrium points given by the set

$$S = \{X \in \mathbb{R}^5 : x_1 = x_2 = x_3 = 0, x_4 = k, x_5 = -k, \text{ where } k \in \mathbb{R}\}. \quad (6)$$

Hence, the new 5-D hyperchaotic system (1) exhibits hidden hyperchaotic attractors. Figure 1 depicts the 2-D MATLAB plots of the attractor of the new

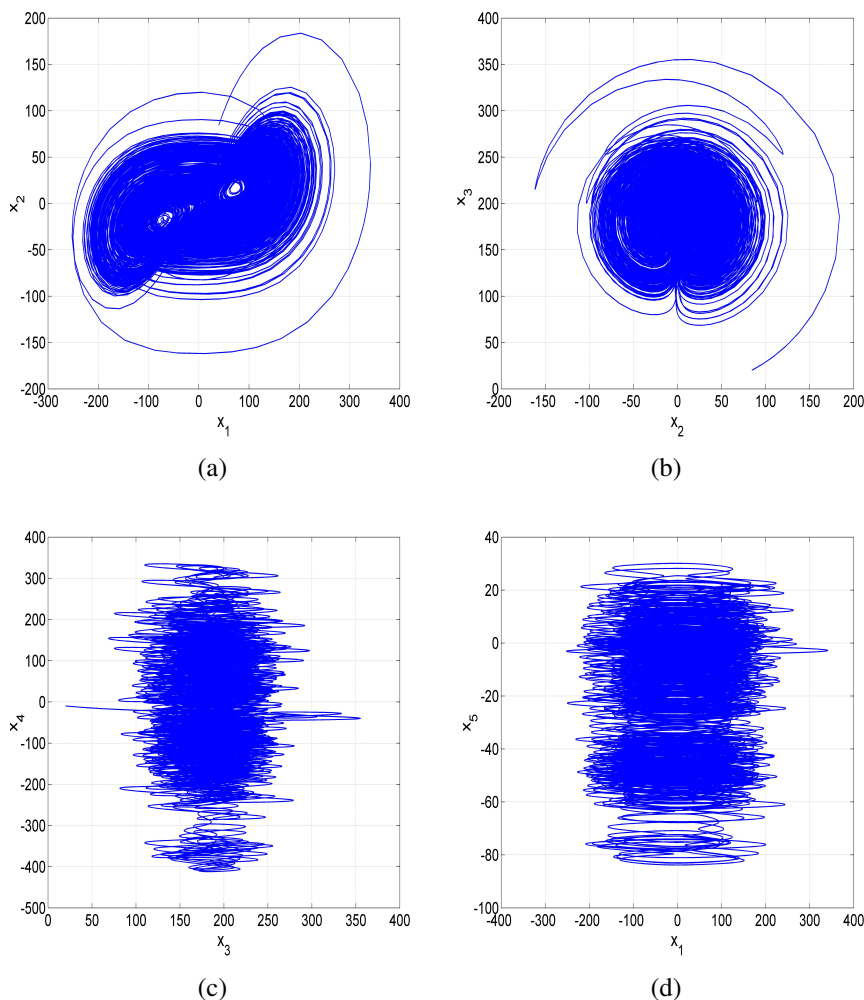


Figure 1: 2-D MATLAB plots of the attractor of the new highly hyperchaotic system (1) for the initial state $(0.2, 0.1, 0.2, 0.1, 0.2)$ and the bifurcation constants $a = 49$, $b = 8$, $c = 180$ and $p = 6$

highly hyperchaotic system (1) for the initial state $(0.2, 0.1, 0.2, 0.1, 0.2)$ and the bifurcation constants $a = 49$, $b = 8$, $c = 180$ and $p = 6$.

3. Bifurcation analysis of the new 5-D hyperchaotic system

In this section, we extend the analysis of the 3-D Vallis model [18], the 4-D hyperchaotic Vaidyanathan system [19] and the 5-D hyperchaotic Vaidyanathan system [20] to investigate a related 5-D hyperchaotic system. We include a quadratic terms in the first equation of the new system and produce phase plots and bifurcation transition diagrams. Then we consider three extensions in which we remove this quadratic term; then include it in the third equation of the system; finally we include the same nonlinear term in both the first and third equations. We find chaotic states in all four systems. The sole equilibrium state in the original system [20] can undergo a Hopf bifurcation for certain parameter choices. This is verified numerically.

3.1. Dissipativity of the 5-D hyperchaotic system

We consider the new five-dimensional system in the form:

$$\dot{x}_1 = -ax_1 + qx_2 + x_2x_3 + x_3 + x_4 + x_5, \quad (7a)$$

$$\dot{x}_2 = cx_1 - x_1x_3 + x_4 + x_5, \quad (7b)$$

$$\dot{x}_3 = -bx_3 + x_1x_2, \quad (7c)$$

$$\dot{x}_4 = -p(x_1 + x_2), \quad (7d)$$

$$\dot{x}_5 = -x_1. \quad (7e)$$

The new 5-D hyperchaotic system (7) extends the 4-D hyperchaotic Vaidyanathan system [19] and modifies the 5-D hyperchaotic Vaidyanathan system [20].

We consider two situations: (i) $a = q$ (as for the chosen set of parameter values); and (ii) $a \neq q$ (as in [20]). We provide the analysis for case (ii) and then see the consequences of case (i). All of the parameter values a, b, c, p, q are taken to be positive.

The divergence of the five-D hyperchaotic system (7) is:

$$\frac{\partial \dot{x}_1}{\partial x_1} + \frac{\partial \dot{x}_2}{\partial x_2} + \frac{\partial \dot{x}_3}{\partial x_3} + \frac{\partial \dot{x}_4}{\partial x_4} + \frac{\partial \dot{x}_5}{\partial x_5} = -(a + b). \quad (8)$$

We therefore require $a + b > 0$ for contracting flows; the flow is divergence-free if $a = -b$.

For the chosen set of parameter values $(a, b, c, q, p) = (49, 8, 180, 49, 6)$ (hyperchaotic case), the divergence of the flow equals -57 which shows that the 5-D hyperchaotic system (7) is dissipative and the volumes are strongly contracting in phase space.

3.2. Linear stability analysis

The equilibrium states are found by setting the RHS of (7) to zero. This gives a line of equilibrium states $(x_1, x_2, x_3, x_4, x_5) = (0, 0, 0, k, -k)$, for some constant k . Its linear stability is found by computing the Jacobian matrix, evaluated at this equilibrium value:

$$J = \begin{pmatrix} -a & q & 1 & 1 & 1 \\ c & 0 & 0 & 1 & 1 \\ 0 & 0 & -b & 0 & 0 \\ -p & -p & 0 & 0 & 0 \\ -1 & 0 & 0 & 0 & 0 \end{pmatrix}, \quad (9)$$

and then determining the roots of the characteristic equation:

$$\lambda(\lambda + b)f(\lambda) = 0, \quad (10)$$

where

$$f(\lambda) = \lambda^3 + a\lambda^2 + (1 + 2p - cq)\lambda + (p(q + c + a) + q). \quad (11)$$

Two eigenvalues are therefore $\lambda = 0$ and $\lambda = -b$, leaving a cubic polynomial $f(\lambda)$ to determine the remaining three eigenvalues. The presence of a zero eigenvalue indicates a degeneracy. The 5-D hyperchaotic Vaidyanathan system [20]) also has this same degeneracy, but not the original 4-D hyperchaotic Vaidyanathan model [19].

3.3. Bifurcation analysis of the 5-D hyperchaotic system

We focus on the remaining eigenvalues of the cubic polynomial $f(\lambda)$. We see that a second eigenvalue $\lambda = 0$ when the constant term $p(q + c + a) + q = 0$. However since all parameters are assumed to be positive, this cannot vanish here. This holds for both cases (i) $(a = q)$ and (ii) $(a \neq q)$. For a Hopf bifurcation, $\lambda = \pm i\omega$, we require

$$\omega^2 = \frac{p(a + q + c) + q}{a} = (1 + 2p - cq) > 0 \quad (12)$$

so that $\frac{1 + 2p}{q} > c$. Combining these two equalities, we obtain the Hopf bifurcation curve

$$pc = (a - q)(1 + p) - caq. \quad (13)$$

When $a = q$, the first factor is zero. Cancelling c from the remaining two terms gives $p = -a^2$. For positive parameters this cannot be satisfied. Therefore a Hopf bifurcation cannot occur. However, when $a \neq q$, we have the possibility of Hopf bifurcations along the curve

$$c = \frac{(1+p)(a-q)}{p+aq}, \quad (14)$$

in terms of c , provided $a > q$. The remaining root of the cubic characteristic equation is $\lambda = -a$. We demonstrate below in Figure 2 that this is an example of a Hopf bifurcation. It is for this reason that we introduced the modified system with $a \neq q$. For the choice of parameter values of $(a, q, b, c, p) = (49, 49, 8, 180, 6)$, the second inequality in the expression for $\omega^2 = -8807$, violating this relation. we therefore explore different parameter choices. One such choice is $(a, q, b, c, p) = (3, 2, 8, 6)$. When c is used as the bifurcation parameter, Figure 1 shows the bifurcation transition diagram of the maxima of $x_{1\max}$ as c decreases from $c = 50$. There are a series of windows of chaotic dynamics for $c > 23.5$, which then gives rise to a series of multiple periodic branches with decreasing periodicity as c decreases. These branches disappear, leaving a single branch which undergoes the Hopf bifurcation at $c = 7/12 \approx 0.5833$. The fixed point analysis above gives $x_4 = k$ and $x_5 = -k$ for some k . Our numerical integrations give $k = 1.20784083E + 004$, in agreement with this result.

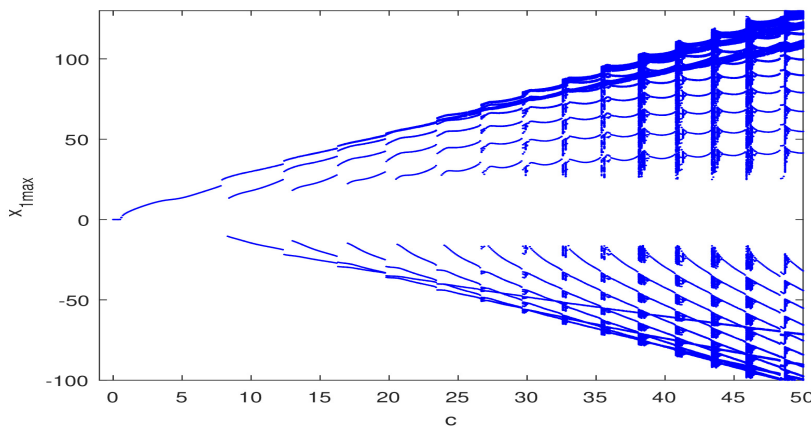


Figure 2: Part of the bifurcation transition plot of $x_{1\max}$ as c decreases for $a = 3$, $q = 2$, $b = 8$ and $p = 6$. There is a Hopf bifurcation at $c = 7/12 \approx 0.5833$

Figure 3 shows the bifurcation transition plots when a decreases from $a = 50$ (upper panel) and a increases from $a = 0$ (lower panel) for $(q, b, c, p) =$

(2, 8, 8, 6). There is hysteresis, and so, multiple nonlinear states for $a < 43$; these states can be either periodic or chaotic.

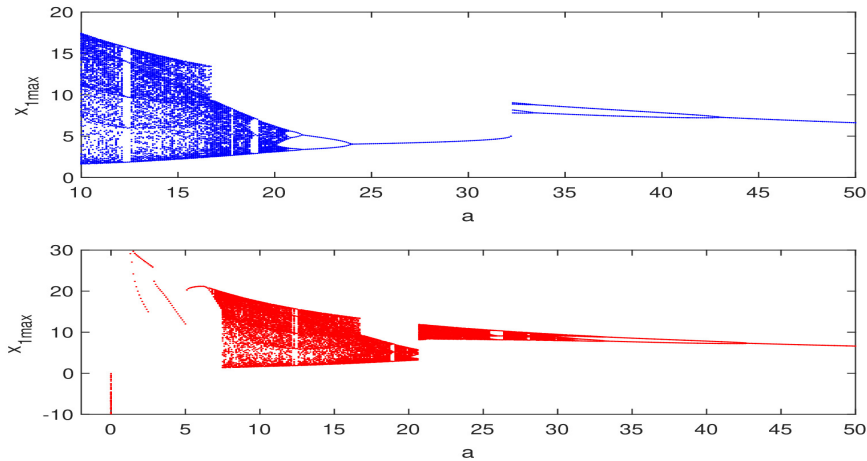


Figure 3: Part of the bifurcation transition plot of x_{\max} as a decreases and increases for $q = 2$, $b = 8$, $c = 8$ and $p = 6$. Solutions become unbounded as $a \rightarrow 0$

Figure 4 shows the bifurcation transition diagram as a decreases for the given choice of parameter values $(q, b, c, p) = (49, 8, 180, 6)$. The dynamics is chaotic throughout. An example of this is shown in Figure 5 for $a = 2$.

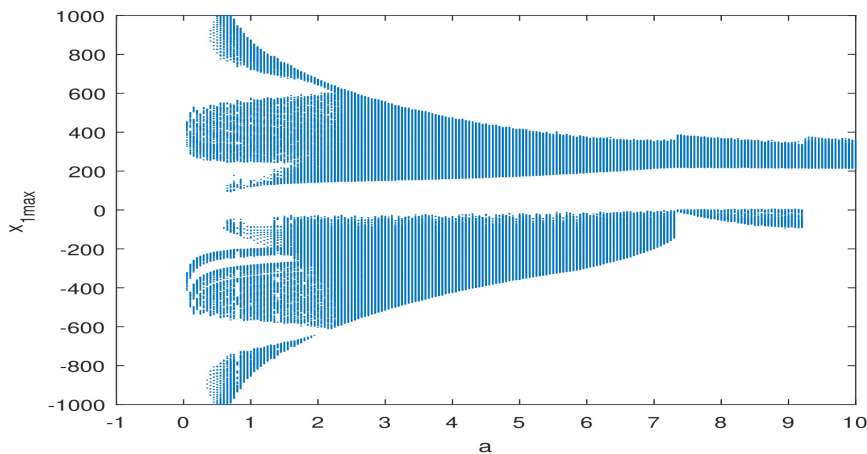


Figure 4: Bifurcation transition plot of $x_{1\max}$ as a decreases for $q = 49$, $c = 180$, $b = 8$, $p = 6$. Note the large values for $x_{1\max}$ as $a \rightarrow 0$

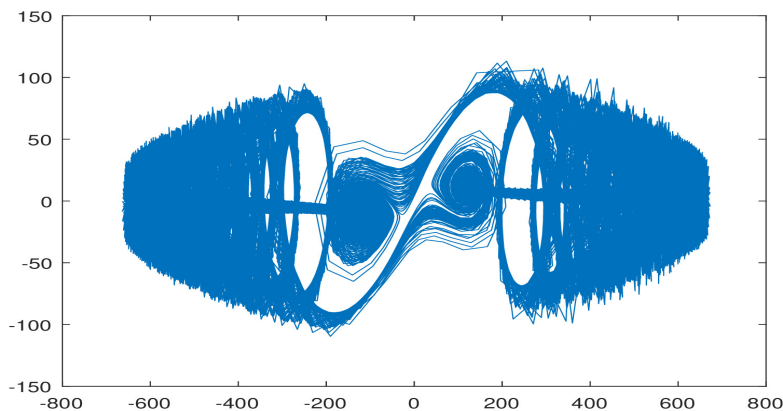


Figure 5: Phase portrait of x_1 vs x_2 for $a = 2$, $q = 49$, $c = 180$, $b = 8$, $p = 6$

3.4. Related 5-D systems

Although the amplitude of x_1 , as shown in Figure 4, as a decreases is very large, the presence of a nonlinear term x_2x_3 in the equation for \dot{x}_1 means we cannot consider the dynamics of this 5-dimensional system at infinity, unlike the system discussed in [20] (We are unable to take the limit as the rescaled variable goes to zero, because that limit is infinity). Figure 6a shows the corresponding

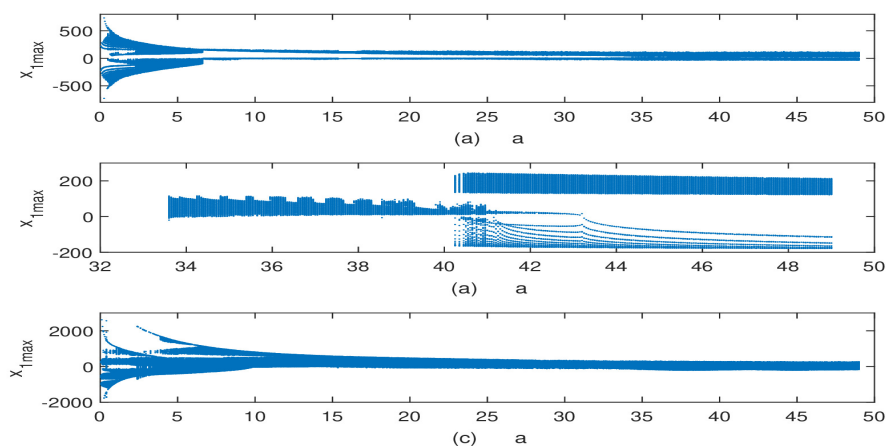


Figure 6: Bifurcation transition plot of $x_{1\max}$ as a decreases for $q = 49$, $c = 180$, $b = 8$, $p = 6$ when (a) the nonlinear term x_2x_3 in the \dot{x}_1 equation is absent; (b) the nonlinear term in the \dot{x}_1 equation is absent, but is added to the \dot{x}_3 ; (c) when the nonlinear term x_2x_3 is included in both equations for \dot{x}_1 and \dot{x}_3 . Note the large values for $x_{1\max}$ as $a \rightarrow 0$ in both (b) and (c)

plot to Figure 4 when this nonlinear term is absent, while Figure 7 shows the corresponding phase portrait to Figure 5. Now it would be possible to analyse the dynamics at infinity, following the same procedure as covered in [20]).

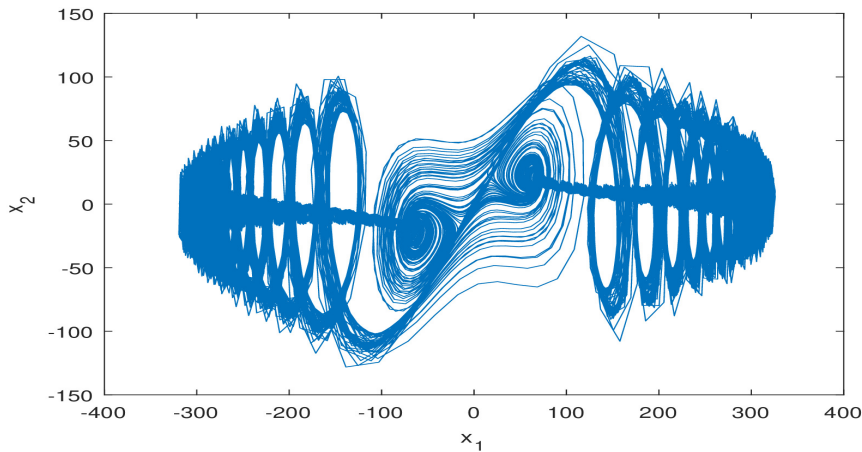


Figure 7: Phase portrait of x_1 vs x_2 for $a = 2$, $q = 49$, $c = 180$, $b = 8$, $p = 6$ when the nonlinear term in the \dot{x}_1 equation is absent

The original Vallis model had an additional $-x_2$ term on the rhs of the equation for \dot{x}_2 . When this is included, the chaos disappears and we are left with a periodic state, as shown in Figure 8.

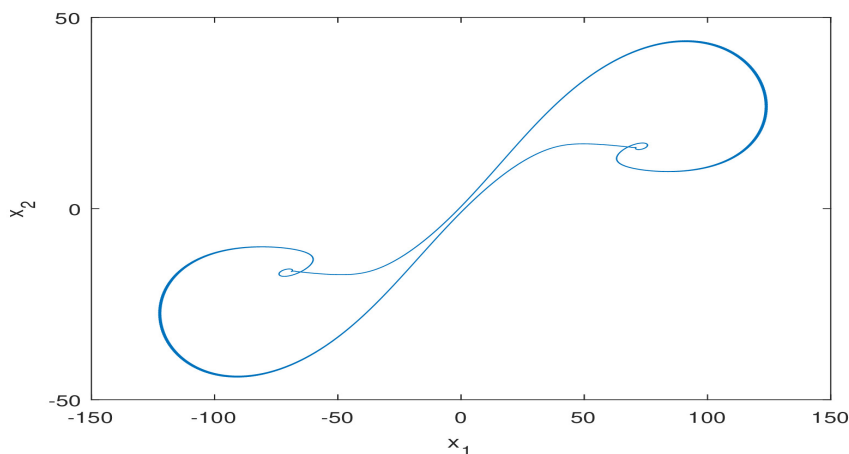


Figure 8: Phase portrait of x_1 vs x_2 for $a = 49$, $q = 49$, $c = 180$, $b = 8$, $p = 6$ when we include a term $-cx_2$ in the equation for \dot{x}_2

If we remove the quadratic term x_2x_3 from the rhs of the \dot{x}_1 equation and place it on the RHS of the \dot{x}_3 equation we obtain the bifurcation transition diagram shown in Figure 6b. This plot should be compared with those of Figure 4. Finally Figure 6c shows the bifurcation transition plots when the same nonlinear term x_2x_3 is included in both \dot{x}_1 and \dot{x}_3 equations. Figure 9 shows two phase portraits for this second case, while Figure 10 shows two phase portraits for $a = 5$ and $a = 15$ from Figure 6c.

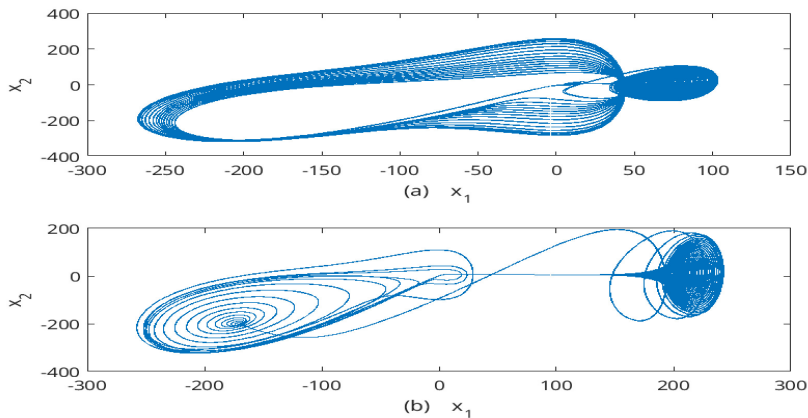


Figure 9: Phase portrait of x_1 vs x_2 for $q = 49$, $c = 180$, $b = 8$, $p = 6$ when we exclude the quadratic term in the \dot{x}_1 equation, but include a term x_2x_3 in the equation for \dot{x}_3 . The upper plot (a) is for $a = 34$ and the lower plot (b) is for $a = 41$

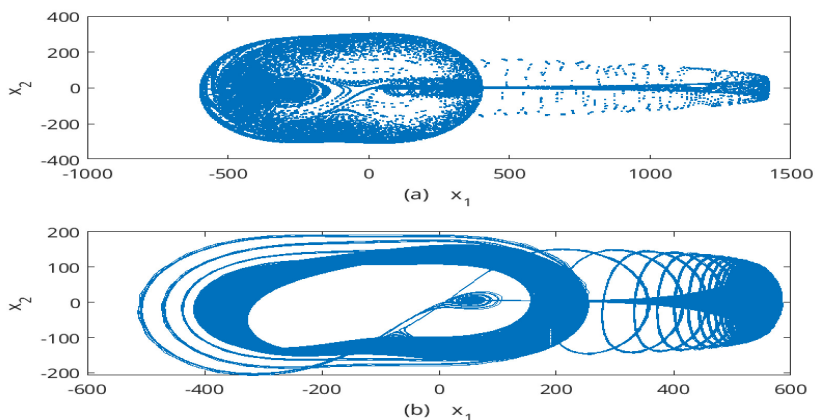


Figure 10: Phase portrait of x_1 vs x_2 for $q = 49$, $c = 180$, $b = 8$, $p = 6$ when we include the same quadratic term x_2x_3 in both the \dot{x}_1 and \dot{x}_3 equations. The upper plot (a) is for $a = 5$ and the lower plot (b) is for $a = 15$

3.5. Summary of the bifurcation analysis of the 5-D hyperchaotic system

The new 5-D hyperchaotic system (7) can support Hopf bifurcations, but not for the initially prescribed parameter values of $(a, b, c, p) = (49, 8, 180, 6)$. Following the analysis in the 4-D Vaidyanathan system (weather fluctuations model) [19] and its extension to the 5-D Vaidyanathan system (weather fluctuations model) [20], we were obliged to introduce an additional parameter q into the \dot{x}_1 equation, so that the terms in x_1 and x_2 have different coefficients. This enables a Hopf bifurcation to occur for much smaller parameter values than the original choice. The Hopf bifurcation are most readily seen in the bifurcation transition diagrams for x_1 max as the parameter c decreases. The value agrees with the results of the linear stability theory.

The bifurcation transition diagrams for the 5-D system, as a decreases, and increases show both periodic and chaotic branches (see Figure 3), with hysteresis and so multiple solutions.

The earlier studies of both Vaidyanathan et al [19] and Vaidyanathan et al [20] had no nonlinear term in the equation for \dot{x}_1 , so that the dynamics at infinity could be investigated. This cannot be undertaken here. However we enclose two plots of the case when this nonlinear term is absent. Both plots bear strong similarities to the new 5-D system (7). As well as removing the quadratic term in the \dot{x}_1 equation, we also included a term in x_2x_3 in the \dot{x}_3 equation. Again chaotic states were observed.

4. Dynamic analysis of the 5-D hyperchaotic system

In this section, we investigate numerically the dynamical analysis of the highly hyperchaotic system (1) using the LE spectrum and bifurcation diagrams. Numerical simulations show that when $a \in [40, 60]$, $b \in [0, 10]$, $c \in [170, 190]$ and $p \in [0, 10]$, the qualitative behaviour of the 5-D system (1) is either periodic, chaotic or hyperchaotic.

4.1. Varying the parameter a

We fix the values of the parameters as $b = 8$, $c = 180$ and $p = 6$. We allow a to vary in the range $[40, 60]$. Figure 11 shows the LE spectrum and the bifurcation diagram of the new 5-D system (1) with respect to the parameter a .

From Figure 11, we can see that the 5-D system (1) is hyperchaotic with three positive Lyapunov exponents ($L_{1,2,3} > 0$), $L_4 = 0$ and $L_5 < 0$. The high value of MLE (L_1) indicates extreme complexity of the 5-D dynamics (1).

The values of Lyapunov exponents when $a = 41.25$ are:

$$L_1 = 7.084, \quad L_2 = 0.04984, \quad L_3 = 0.01297, \quad L_4 = 0, \quad L_5 = -56.39. \quad (15)$$

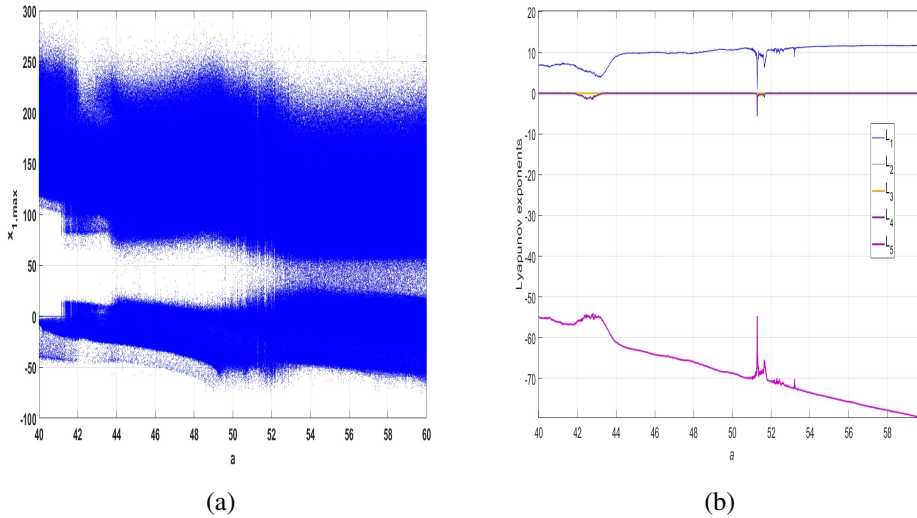


Figure 11: (a) Bifurcation diagram and (b) LE spectrum of the 5-D dynamics (1) for $a \in [40, 60]$, $b = 8$, $c = 180$ and $p = 6$

The values of Lyapunov exponents when $a = 44.5$ are:

$$L_1 = 9.705, \quad L_2 = 0.07931, \quad L_3 = .017770, \quad L_4 = 0, \quad L_5 = -62.30. \quad (16)$$

The values of Lyapunov exponents when $a = 50$ are:

$$L_1 = 10.70, \quad L_2 = 0.060, \quad L_3 = 0.01362, \quad L_4 = 0, \quad L_5 = -68.79. \quad (17)$$

The values of Lyapunov exponents when $b = 58.60$ are:

$$L_1 = 11.73, \quad L_2 = 0.0701, \quad L_3 = 0.0062, \quad L_4 = 0, \quad L_5 = -78.41. \quad (18)$$

4.2. Varying the parameter b

We fix the values of the parameters as $a = 49$, $c = 180$ and $p = 6$. We allow b to vary in the range $[0, 10]$. Figure 12 shows the LE spectrum and the bifurcation diagram of the new 5-D system (1) with respect to the parameter b .

When $b \in [0, 0.13]$, the MLE of the new 5-D system (1) is zero, implying that system (1) displays periodic behavior with no complexity. When we chose the control parameter as $b = 0.06$, the corresponding Lyapunov exponents are:

$$L_1 = 0, \quad L_2 = 0, \quad L_3 = -1.3893, \quad L_4 = -1.5901, \quad L_5 = -46.0774. \quad (19)$$

The values of Lyapunov exponents when $b = 0.12$ are:

$$L_1 = 0, \quad L_2 = 0, \quad L_3 = -0.2965, \quad L_4 = -0.3942, \quad L_5 = -48.4229. \quad (20)$$

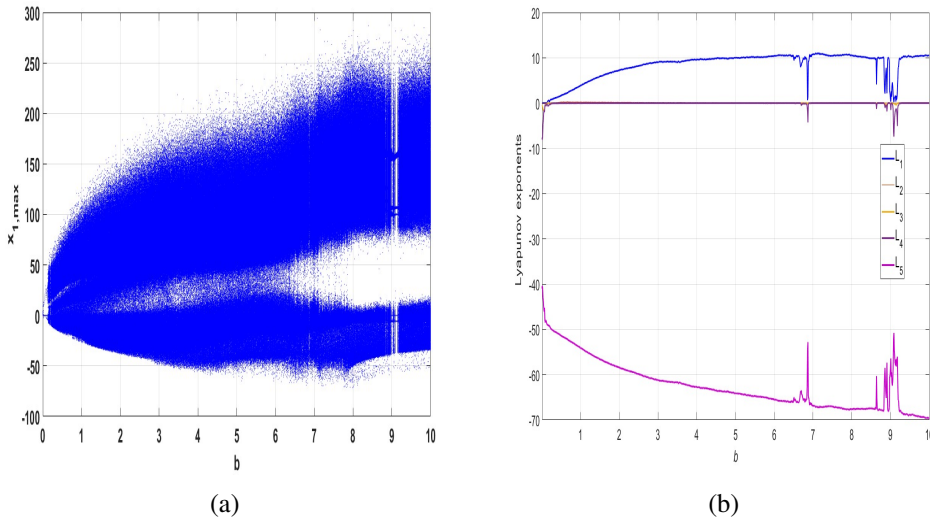


Figure 12: (a) Bifurcation diagram and (b) LE spectrum of the 5-D dynamics (1) for $b \in [0, 10]$, $a = 49$, $c = 180$ and $p = 6$

When $b \in (0.13, 0.25] \cup [9, 9.17]$, from Figure 12 we can see that there is one positive Lyapunov exponent, implying that the system (1) displays chaotic behavior. When we choose the control parameter $b = 0.15$, the corresponding Lyapunov exponents are:

$$L_1 = 0.4275, \quad L_2 = 0, \quad L_3 = 0, \quad L_4 = -0.60142, \quad L_5 = -48.9764. \quad (21)$$

The values of Lyapunov exponents when $b = 0.22$ are:

$$L_1 = 0.6992, \quad L_2 = 0, \quad L_3 = 0, \quad L_4 = -0.2402, \quad L_5 = -49.6745. \quad (22)$$

The values of Lyapunov exponents when $b = 9$ are:

$$L_1 = 0.7972, \quad L_2 = 0, \quad L_3 = 0, \quad L_4 = -0.1689, \quad L_5 = -58.6325. \quad (23)$$

When $b \in (0.25, 9) \cup (9.17, 10]$, the system (1) displays hyperchaotic behavior with two and three positive Lyapunov exponents and a very high value of MLE providing extreme complexity of the dynamics (1). When $b = 0.50$, the corresponding Lyapunov exponents are:

$$L_1 = 1.6637, \quad L_2 = 0.2341, \quad L_3 = 0, \quad L_4 = -0.01629, \quad L_5 = -51.3794. \quad (24)$$

The values of Lyapunov exponents when $b = 4$ are:

$$L_1 = 9.6679, \quad L_2 = 0.1317, \quad L_3 = 0, \quad L_4 = -0.2402, \quad L_5 = -62.8030. \quad (25)$$

The values of Lyapunov exponents when $b = 8$ are:

$$L_1 = 10.5380, \quad L_2 = 0, \quad L_3 = 0.0130, \quad L_4 = 0, \quad L_5 = -58.6325. \quad (26)$$

4.3. Varying the parameter c

We fix the values of the parameters as $a = 49$, $b = 8$ and $p = 6$. We allow c to vary in the range $[170, 190]$. Figure 13 shows the LE spectrum and the bifurcation diagram of the new 5-D system (1) with respect to the parameter c .

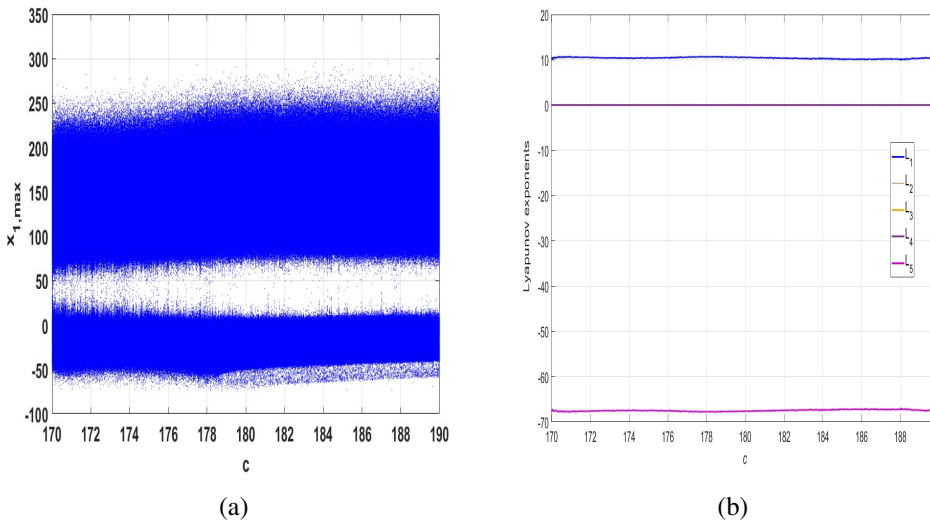


Figure 13: (a) Bifurcation diagram and (b) LE spectrum of the 5-D dynamics (1) for $c \in [170, 190]$, $a = 49$, $b = 8$ and $p = 6$

From Figure 13, we see that the 5-D system (1) is hyperchaotic for $c \in [170, 190]$ with three positive Lyapunov exponents ($L_{1,2,3} > 0$), $L_4 = 0$ and $L_5 < 0$. The high value of MLE (L_1) indicates extreme complexity of the 5-D dynamics (1).

The values of Lyapunov exponents when $c = 171.50$ are:

$$L_1 = 10.58, \quad L_2 = 0.07455, \quad L_3 = 0.01435, \quad L_4 = 0, \quad L_5 = -67.66. \quad (27)$$

The values of Lyapunov exponents when $c = 176$ are:

$$L_1 = 10.37, \quad L_2 = 0.07685, \quad L_3 = 0.01383, \quad L_4 = 0, \quad L_5 = -67.54. \quad (28)$$

The values of Lyapunov exponents when $c = 182$ are:

$$L_1 = 10.31, \quad L_2 = 0.08558, \quad L_3 = 0.01263, \quad L_4 = 0, \quad L_5 = -67.46. \quad (29)$$

The values of Lyapunov exponents when $c = 189$ are:

$$L_1 = 10.25, \quad L_2 = 0.07558, \quad L_3 = 0.01814, \quad L_4 = 0, \quad L_5 = -67.34. \quad (30)$$

4.4. Varying the parameter p

We fix the values of the parameters as $a = 49$, $b = 8$ and $c = 180$. We allow p to vary in the range $[0, 10]$. Figure 14 shows the LE spectrum and the bifurcation diagram of the new 5-D system (1) with respect to the parameter p .

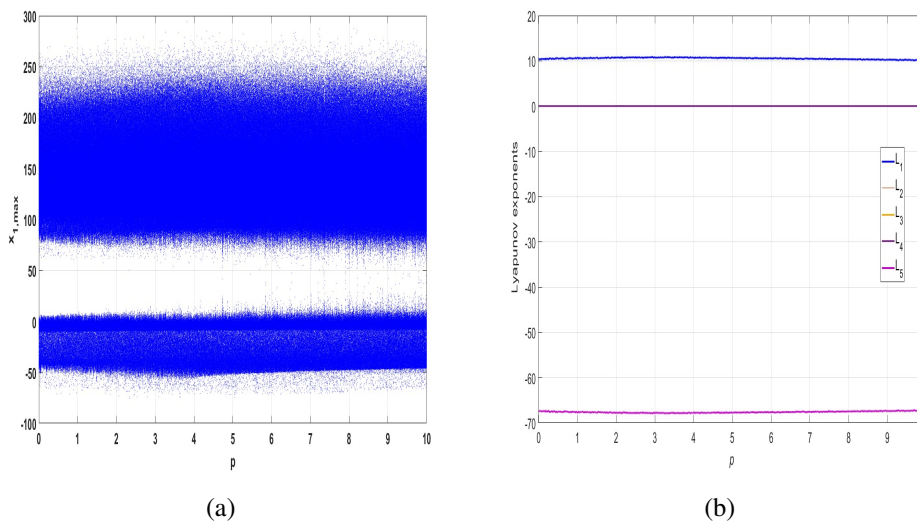


Figure 14: (a) Bifurcation diagram and (b) LE spectrum of the 5-D dynamics (1) for $p \in [0, 10]$, $a = 49$, $b = 8$ and $c = 180$

From Figure 14, we see that the 5-D system (1) is hyperchaotic for $p \in [0, 10]$ with three positive Lyapunov exponents ($L_{1,2,3} > 0$), $L_4 = 0$ and $L_5 < 0$. The high value of MLE (L_1) indicates extreme complexity of the 5-D dynamics (1).

The values of Lyapunov exponents when $p = 1.95$ are:

$$L_1 = 10.72, \quad L_2 = 0.01388, \quad L_3 = 0.02505, \quad L_4 = 0, \quad L_5 = -67.72. \quad (31)$$

The values of Lyapunov exponents when $p = 4$ are:

$$L_1 = 10.62, \quad L_2 = 0.01392, \quad L_3 = 0.05359, \quad L_4 = 0, \quad L_5 = -67.68. \quad (32)$$

The values of Lyapunov exponents when $p = 6$ are:

$$L_1 = 10.54, \quad L_2 = 0.01330, \quad L_3 = 0.07263, \quad L_4 = 0, \quad L_5 = -67.62. \quad (33)$$

The values of Lyapunov exponents when $p = 8.4$ are:

$$L_1 = 10.38, \quad L_2 = 0.01511, \quad L_3 = 0.0957, \quad L_4 = 0, \quad L_5 = -67.48. \quad (34)$$

The values of Lyapunov exponents when $p = 9.65$ are:

$$L_1 = 10.27, \quad L_2 = 0.1273, \quad L_3 = 0.01326, \quad L_4 = 0, \quad L_5 = -67.41. \quad (35)$$

5. Circuit simulation of the new 5d hyperchaotic system

In this section, the new 5D hyperchaotic system (1) is realized by the NI Multisim 14.2 platform. The electronic circuit design of the 5D hyperchaotic system (36) is shown in Figure 15 in which TLO84ACD is selected as OPAMP and the multipliers are of type AD633.

Using Kirchhoff's electrical circuit laws, we derive the circuit model for the rescaled 5D hyperchaotic system (1) as follows:

$$\left\{ \begin{array}{l} \dot{x} = \frac{1}{R_1 C_1} y - \frac{1}{R_2 C_1} x + \frac{1}{10 R_3 C_1} y z + \frac{1}{R_4 C_1} z + \frac{1}{R_5 C_1} v + \frac{1}{R_6 C_1} w, \\ \dot{y} = \frac{1}{R_7 C_2} x + \frac{1}{10 R_8 C_2} x z + \frac{1}{R_9 C_2} v + \frac{1}{R_{10} C_2} w, \\ \dot{z} = \frac{1}{10 R_{11} C_3} x y - \frac{1}{R_{12} C_3} z, \\ \dot{v} = -\frac{1}{R_{13} C_4} x - \frac{1}{R_{14} C_4} y, \\ \dot{w} = -\frac{1}{R_{15} C_5} x, \end{array} \right. \quad (36)$$

Here x, y, z, v, w are the voltages across the capacitors, C_1, C_2, C_3, C_4, C_5 , respectively. The values of components in the circuit are selected as:

$$C_1 = C_2 = C_3 = C_4 = C_5 = 1 \text{ nF}, \quad (37)$$

$$R_1 = R_2 = 2.04 \text{ k}\Omega, \quad R_3 = R_8 = R_{11} = 10 \text{ k}\Omega, \quad R_7 = 1 \text{ k}\Omega, \quad (38)$$

$$R_4 = R_5 = R_6 = R_9 = R_{10} = R_{15} = R_{16} = R_{17} = R_{18} = 100 \text{ k}\Omega, \quad (39)$$

$$R_{19} = R_{20} = R_{21} = R_{22} = R_{23} = R_{24} = R_{25} = 100 \text{ k}\Omega, \quad (40)$$

$$R_{12} = 12.5 \text{ k}\Omega, \quad R_{13} = R_{14} = 16.67 \text{ k}\Omega. \quad (41)$$

Multisim outputs of the 5-D hyperchaotic circuit (36) are presented in Figure 16 via oscilloscope XSC1. Multisim outputs of the 5-D hyperchaotic circuit (36) are presented in Figure 17 via Tektronix oscilloscope.

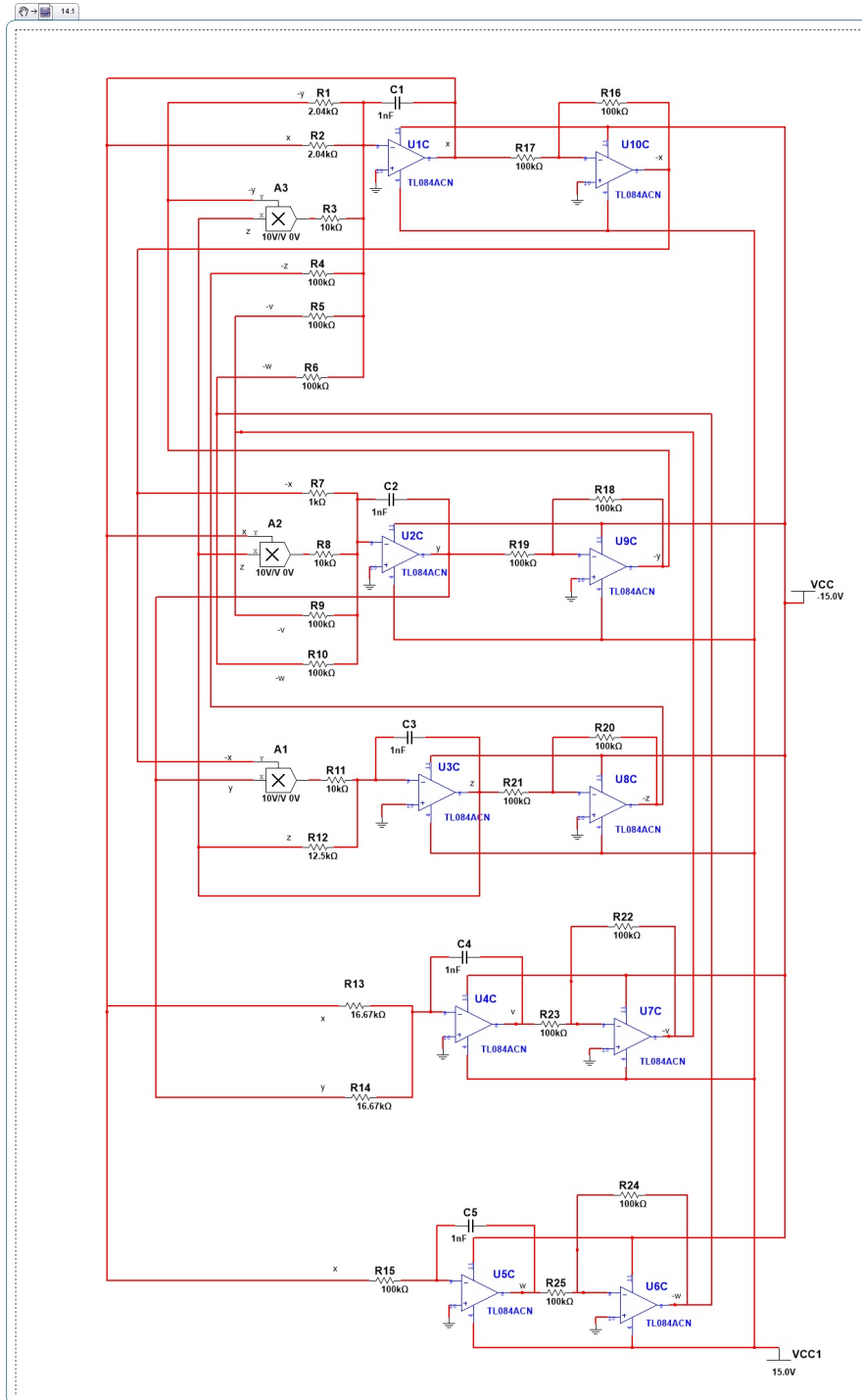
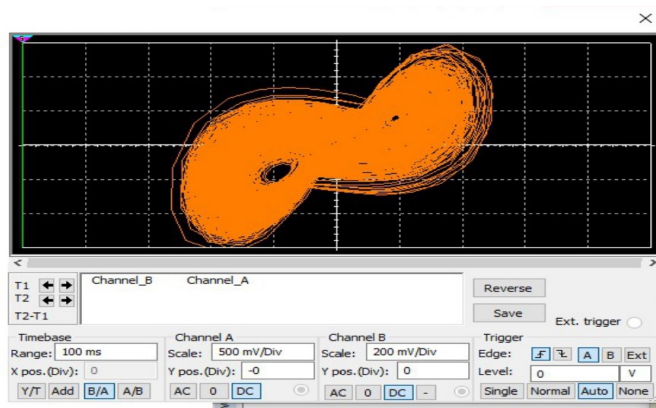
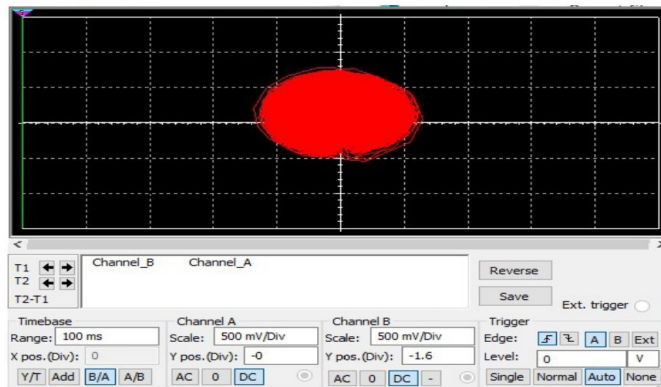


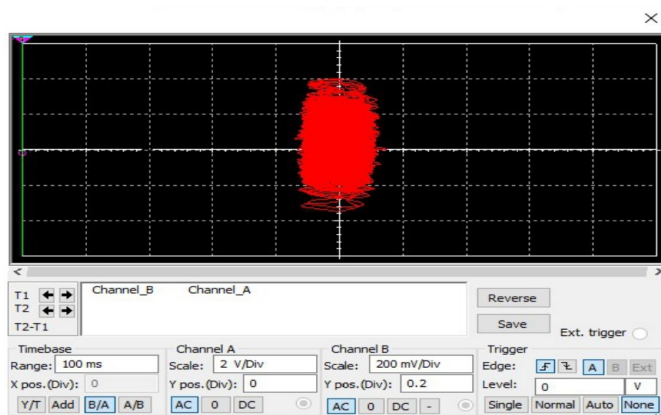
Figure 15: Circuit design of the new 5-D hyperchaotic system (36)



(a)

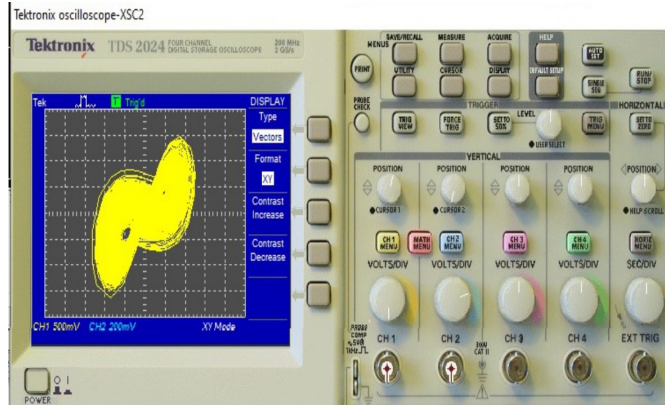


(b)

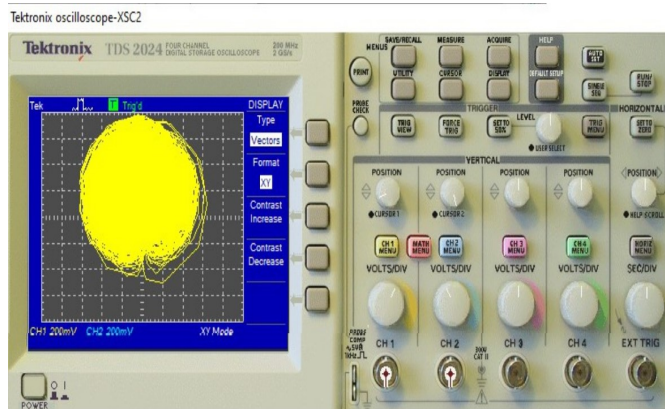


(c)

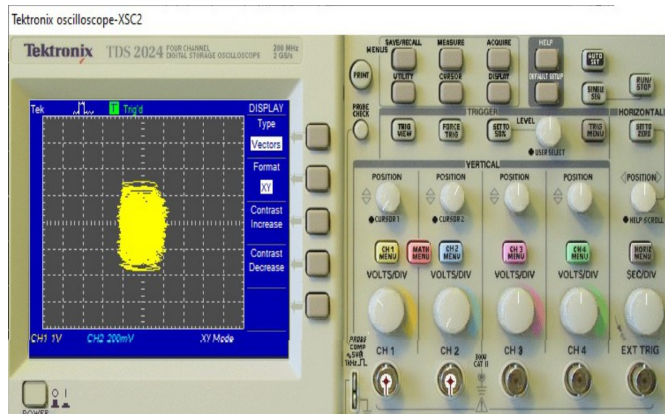
Figure 16: Hyperchaotic attractors of the new 5-D hyperchaotic circuit (36) via oscilloscope XSC1:
(a) (x, y) plane, (b) (y, z) plane and (c) (x, v) plane



(a)



(b)



(c)

Figure 17: Hyperchaotic attractors of the new 5-D hyperchaotic circuit (36) via Tektronix oscilloscope: (a) (x, y) plane, (b) (y, z) plane and (c) (x, v) plane

6. Global stabilization of the 5-D hyperchaotic system via integral sliding mode control

In this section, we apply integral sliding mode control (ISMC) to achieve global stabilization of the new 5-D hyperchaotic system which is introduced in Section 2.

Thus, we consider the 5-D hyperchaotic system with integral sliding mode control defined by

$$\begin{cases} \dot{x}_1 = a(x_2 - x_1) + x_2x_3 + x_3 + x_4 + x_5 + V_1, \\ \dot{x}_2 = cx_2 - x_1x_3 + x_4 + x_5 + V_2, \\ \dot{x}_3 = x_1x_2 - bx_3 + V_3, \\ \dot{x}_4 = -p(x_1 + x_2) + V_4, \\ \dot{x}_5 = -x_1 + V_5. \end{cases} \quad (42)$$

We represent $X = (x_1, x_2, x_3, x_4, x_5)$ as the state of the 5-D hyperchaotic system (42).

We denote $V = (V_1, V_2, V_3, V_4, V_5)$ as the sliding mode controller which is to be designed with an objective to globally stabilize the states of the 5-D hyperchaotic system (42) asymptotically with time.

In the IMSC design, we associate an integral sliding surface with every state error variable x_i , ($i = 1, 2, 3, 4, 5$) as follows:

$$\begin{cases} S_1 = x_1 + \mu_1 \int_0^t x_1(\alpha) d\alpha, \\ S_2 = x_2 + \mu_2 \int_0^t x_2(\alpha) d\alpha, \\ S_3 = x_3 + \mu_3 \int_0^t x_3(\alpha) d\alpha, \\ S_4 = x_4 + \mu_4 \int_0^t x_4(\alpha) d\alpha, \\ S_5 = x_5 + \mu_5 \int_0^t x_5(\alpha) d\alpha. \end{cases} \quad (43)$$

Differentiating the equations given in (43), we obtain:

$$\begin{cases} \dot{S}_1 = \dot{x}_1 + \mu_1 x_1, \\ \dot{S}_2 = \dot{x}_2 + \mu_2 x_2, \\ \dot{S}_3 = \dot{x}_3 + \mu_3 x_3, \\ \dot{S}_4 = \dot{x}_4 + \mu_4 x_4, \\ \dot{S}_5 = \dot{x}_5 + \mu_5 x_5. \end{cases} \quad (44)$$

We suppose that μ_i , ($i = 1, 2, 3, 4, 5$) are positive constants.

We consider the integral sliding mode controls as follows:

$$\begin{aligned} V_1 &= -a(x_2 - x_1) - \mu_1 x_1 - \epsilon_1 \operatorname{sgn}(S_1) - \kappa_1 S_1, \\ V_2 &= -cx_2 + x_1 x_3 - x_4 - x_5 - \mu_2 x_2 - \epsilon_2 \operatorname{sgn}(S_2) - \kappa_2 S_2, \\ V_3 &= -x_1 x_2 + bx_3 - \mu_3 x_3 - \epsilon_3 \operatorname{sgn}(S_3) - \kappa_3 S_3, \\ V_4 &= p(x_1 + x_2) - \mu_4 x_4 - \epsilon_4 \operatorname{sgn}(S_4) - \kappa_4 S_4, \\ V_5 &= x_1 - \mu_5 x_5 - \epsilon_5 \operatorname{sgn}(S_5) - \kappa_5 S_5. \end{aligned} \quad (45)$$

In Eq. (45), μ_i , ϵ_i , κ_i , ($i = 1, 2, 3, 4, 5$) are positive constants.

Substituting (45) into the state dynamics (42), we obtain the following:

$$\begin{cases} \dot{x}_1 = -\mu_1 x_1 - \epsilon_1 \operatorname{sgn}(S_1) - \kappa_1 S_1, \\ \dot{x}_2 = -\mu_2 x_2 - \epsilon_2 \operatorname{sgn}(S_2) - \kappa_2 S_2, \\ \dot{x}_3 = -\mu_3 x_3 - \epsilon_3 \operatorname{sgn}(S_3) - \kappa_3 S_3, \\ \dot{x}_4 = -\mu_4 x_4 - \epsilon_4 \operatorname{sgn}(S_4) - \kappa_4 S_4, \\ \dot{x}_5 = -\mu_5 x_5 - \epsilon_5 \operatorname{sgn}(S_5) - \kappa_5 S_5. \end{cases} \quad (46)$$

We apply Lyapunov stability theory to establish the main control result of this section, which is provided in the following theorem.

Theorem 1. *The integral sliding mode control law (45) globally stabilizes the 5-D hyperchaotic system (42) for all values of initial states $X(0)$ in \mathbb{R}^5 , where it is assumed that μ_i , ϵ_i , κ_i ($i = 1, 2, 3, 4, 5$) are positive constants.*

Proof. We start the proof by taking the Lyapunov function defined by

$$V(S_1, S_2, S_3, S_4, S_5) = \frac{1}{2} (S_1^2 + S_2^2 + S_3^2 + S_4^2 + S_5^2). \quad (47)$$

It is easy to check that V is a quadratic and strictly positive definite function on \mathbb{R}^5 . Next, we find that

$$\dot{V} = S_1 \dot{S}_1 + S_2 \dot{S}_2 + S_3 \dot{S}_3 + S_4 \dot{S}_4 + S_5 \dot{S}_5. \quad (48)$$

A simple calculation shows that

$$\dot{V} = \sum_{i=1}^5 S_i(-\epsilon_i \operatorname{sgn}(S_i) - \kappa_i S_i). \quad (49)$$

It is easy to check that

$$\dot{V} = - \sum_{i=1}^5 [\epsilon_i |S_i| + \kappa_i S_i^2]. \quad (50)$$

Since $\epsilon_i > 0$ and $\kappa_i > 0$ for $i = 1, 2, 3, 4, 5$, \dot{V} is a negative definite function defined on \mathbb{R}^5 .

Using Lyapunov stability theory [17], we deduce that $S_i(t) \rightarrow 0$, ($i = 1, 2, 3, 4, 5$) as $t \rightarrow \infty$.

Hence, it follows that $x_i(t) \rightarrow 0$, ($i = 1, 2, 3, 4, 5$) as $t \rightarrow \infty$.

This completes the proof. \square

For MATLAB simulations, the constants are considered as in the hyperchaos case, *viz.* $a = 49$, $b = 8$, $c = 180$ and $p = 6$.

Let us assume the sliding constants as $\epsilon_i = 0.2$, $\kappa_i = 16$ and $\mu_i = 12$ for $i = 1, 2, 3, 4, 5$.

The initial state of the 5-D hyperchaotic system (42) is taken as

$$x_1(0) = 6.4, \quad x_2(0) = 1.2, \quad x_3(0) = 4.7, \quad x_4(0) = 2.3, \quad x_5(0) = 8.5. \quad (51)$$

Figure 18 illustrates the global asymptotic stabilization of the 5-D hyperchaotic system (42) using integral sliding mode control (ISMC).

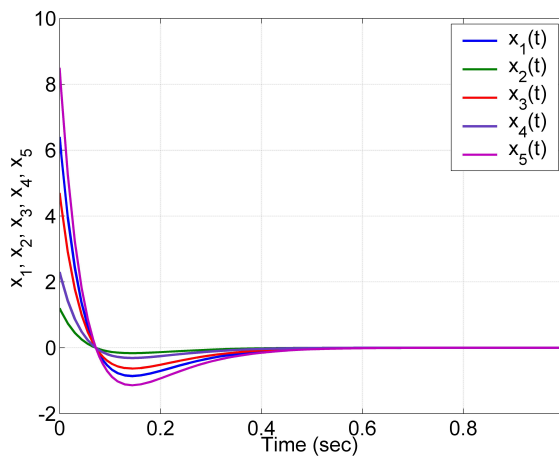


Figure 18: MATLAB plot showing the asymptotic stabilization of the 5-D hyperchaotic system (42) using ISMC

7. Conclusions

In this research work, we contributed a new 5-D highly hyperchaotic system with three quadratic nonlinear terms. A novel feature of the proposed hyperchaotic system is that it has the maximal Lyapunov exponent (MLE) given by $L_1 = 10.5374$ showing that the 5-D hyperchaotic system has high complexity. Another novel feature of the new hyperchaotic system is that the system exhibits a line of equilibrium points, which shows that the 5-D hyperchaotic system has hidden attractors. We carried out a detailed bifurcation analysis of the new hyperchaotic system with a line equilibrium. Using Multisim, we had also built an electronic circuit of the new 5-D hyperchaotic system with a line equilibrium. As a control application, we applied integral sliding mode control (ISMC) to achieve global asymptotic stabilization of the new 5-D highly hyperchaotic system with a line equilibrium. Lyapunov control theory was applied to establish the stabilization results for the new 5-D hyperchaotic system. MATLAB simulation results were presented to illustrate the main results of this research work.

References

- [1] S. VAIDYANATHAN and A.T. AZAR: *Backstepping Control of Nonlinear Dynamical Systems*, Academic Press, New York, 2020.
- [2] H. GAO, G. ZHENG and T. GAO: A secure image encryption-sharing based on different diffusion intensities by hyper-chaos according to image features. *Signal, Image and Video Processing*, **18**(11), (2024), 8119–8130. DOI: [10.1007/s11760-024-03455-z](https://doi.org/10.1007/s11760-024-03455-z)
- [3] T. LI, X. TONG, M. ZHANG and Z. WANG: Image encryption algorithm based on DNA mutation and a novel four-dimensional hyperchaos. *Physica Scripta*, **99**(10), (2024), Article ID 105210. DOI: [10.1088/1402-4896/ad7239](https://doi.org/10.1088/1402-4896/ad7239)
- [4] J. XU, X. ZHANG and S. ZHONG: Hidden complex multistable dynamical analysis and FPGA implementation of integer-fractional order memristive-memcapacitive chaotic system. *Physica Scripta*, **99**(12), (2024), Article ID 125248. DOI: [10.1088/1402-4896/ad8f76](https://doi.org/10.1088/1402-4896/ad8f76)
- [5] I. HUSSAN, M. ZHAO and X. ZHANG: Two-memristor-based maps with infinitely many hyperchaotic attractors. *Chaos, Solitons and Fractals*, **191** (2025), Article ID 115904. DOI: [10.1016/j.chaos.2024.115904](https://doi.org/10.1016/j.chaos.2024.115904)
- [6] H. HUA, Q. LAI, Y. ZHANG, S. BANERJEE and S. JAFARI: High robustness image encryption scheme utilizing memristive hyperchaotic map and Manhattan distance. *Nonlinear Dynamics*, **113**(2), (2025), 1857–1878. DOI: [10.1007/s11071-024-10284-9](https://doi.org/10.1007/s11071-024-10284-9)
- [7] Y. LUO, Q. LIU, X. CHE and Z. HE: LMF algorithm based on hyper-chaos for the solving of forward displacement in a parallel robot mechanism. *International Journal of Advanced Robotic Systems*, **10** (2013), Article ID 30. DOI: [10.5772/54817](https://doi.org/10.5772/54817)
- [8] M.S. AZZAZ, R. KAIBOU and B. MADANI: Co-design based FPGA implementation of an efficient new speech hyperchaotic cryptosystem in the transform domain. *Integration*, **97** (2024), Article ID 102197. DOI: [10.1016/j.vlsi.2024.102197](https://doi.org/10.1016/j.vlsi.2024.102197)

- [9] S.Y. LI, G.Y. WU, J.Y. SUN, P.F. YAN and H. ZHANG: Novel 3D-PCHCS design and application on ophthalmic medical image copyright protection with FPGA implementation. *Journal of Real-Time Image Processing*, **22**(1), (2025), Article ID 33. DOI: [10.1007/s11554-024-01609-3](https://doi.org/10.1007/s11554-024-01609-3)
- [10] S. VAIDYANATHAN and C. VOLOS: *Advances and Applications in Nonlinear Control Systems*, Springer, New York, 2016.
- [11] T. MA, J. MOU and W. CHEN: Dynamics and implementation of a functional neuron model with hyperchaotic behavior under electromagnetic radiation. *Chaos, Solitons and Fractals*, **190** (2025), Article ID 115795. DOI: [10.1016/j.chaos.2024.115795](https://doi.org/10.1016/j.chaos.2024.115795)
- [12] J. ZHANG and E. LIU: Design and synchronization control application of a new five-dimensional memristor CNN conservative hyperchaotic system. *Physica Scripta*, **99**(12), (2024), Article ID 125246. DOI: [10.1088/1402-4896/ad8e96](https://doi.org/10.1088/1402-4896/ad8e96)
- [13] G. VIVEKANANDHAN, J.C. CHEDJOU, J. KENGNE and K. RAJAGOPAL: A unique self-driven 5D hyperjerk circuit with hyperbolic sine function: Hyperchaos with three positive exponents, complex transient behavior and coexisting attractors. *Chaos, Solitons and Fractals*, **186** (2024), Article ID 115276. DOI: [10.1016/j.chaos.2024.115276](https://doi.org/10.1016/j.chaos.2024.115276)
- [14] S. MOBAYEN, J. MOSTAFAEE, K.A. ALATTAS, M.T. KE, Y.H. HSUEH and A. ZHILENKOV: A new hyperchaotic system: circuit realization, nonlinear analysis and synchronization control. *Physica Scripta*, **99**(10), (2024), Article ID 105204. DOI: [10.1088/1402-4896/ad71fc](https://doi.org/10.1088/1402-4896/ad71fc)
- [15] W. ZHU, K. SUN, H. WANG, L. FU and L. MINATI: Dynamics, synchronization and analog circuit implementation of a discrete neuron-like map with pulsating spiral dynamics. *Chaos, Solitons and Fractals*, **186** (2024), Article ID 115281. DOI: [10.1016/j.chaos.2024.115281](https://doi.org/10.1016/j.chaos.2024.115281)
- [16] S. VAIDYANATHAN, I.M. MOROZ and A. SAMBAS: A new two-scroll 4-D hyperchaotic system with a unique saddle point equilibrium, its bifurcation analysis, circuit design and a control application to complete synchronization. *Archives of Control Sciences*, **33**(2), (2023), 277–298. DOI: [10.24425/acs.2023.146276](https://doi.org/10.24425/acs.2023.146276)
- [17] W.M. HADDAD and V. CHELLABOINA: *Nonlinear Dynamical Systems and Control: A Lyapunov-Based Approach*. Princeton University Press, Princeton, USA, 2008.
- [18] G.K. VALLIS: El Nino: a chaotic dynamical system. *Science*, **232**(4747), (1986), 243–245. DOI: [10.1126/science.232.4747.243](https://doi.org/10.1126/science.232.4747.243)
- [19] S. VAIDYANATHAN, A.T. AZAR, K. RAJAGOPAL, A. SAMBAS, S. KACAR and U. CAVUSOGLU: A new hyperchaotic temperature fluctuations model, its circuit simulation, FPGA implementation and an application to image encryption. *International Journal of Simulation and Process Modelling*, **13**(3), (2018), 281–296. DOI: [10.1504/IJSPM.2018.093113](https://doi.org/10.1504/IJSPM.2018.093113)
- [20] S. VAIDYANATHAN, I.M. MOROZ, E. TLELO-CUAUTLE, A. SAMBAS, C.F. BERMUDEZ and S.A. SAFAN: Mathematical modelling, bifurcation analysis, circuit design and FPGA implementation of a 5D hyperchaotic weather fluctuation model with a line of equilibrium points. *International Journal of Modelling, Identification and Control*, **43**(4), (2023), 267–283. DOI: [10.1504/IJMIC.2023.10059035](https://doi.org/10.1504/IJMIC.2023.10059035)